PROCEEDINGS OF THE ROYAL SOCIETY B

Proc. R. Soc. B (2005) **272**, 957–962
doi:10.1098/rspb.2004.2993
Published online 7 May 2005

Scaling of mammalian ethmoid bones can predict olfactory organ size and performance

Henry Pihlström[1,*], Mikael Fortelius[2], Simo Hemilä[1], Roger Forsman[4] and Tom Reuter[3]

[1]*Department of Biosciences,* [2]*Department of Geology and Institute of Biotechnology, and* [3]*Department of Ecology and Systematics, University of Helsinki, PO Box 64, FIN-00014 Helsinki, Finland*
[4]*Leivosbölevägen 61, 02510 Oitbacka, Finland*

The relation between size and performance is central for understanding the evolution of sensory systems, and much interest has been focused on mammalian eyes and ears. However, we know very little about olfactory organ size (OOS), as data for a representative set of mammals are lacking. Here, we present a cranial endocast method for estimating OOS by measuring an easily accessible part of the system, the perforated part of the ethmoid bone, through which the primary olfactory axons reach the olfactory bulb. In 16 species, for which relevant data are available, the area of the perforated ethmoid bone is directly proportional to the area of the olfactory epithelium. Thus, the ethmoid bone is a useful indicator enabling us to analyse 150 species, and describe the distribution of OOS within the class Mammalia. In the future, a method using skull material may be applied to fossil skulls. In relation to skull size, humans, apes and monkeys have small olfactory organs, while prosimians have OOSs typical for mammals of their size. Large ungulates have impressive olfactory organs. Relating anatomy to published thresholds, we find that sensitivity increases with increasing absolute organ size.

Keywords: mammals; olfactory organ size; ethmoid bone; endocasts; primates

1. INTRODUCTION

The nasal cavity, the olfactory epithelium and the olfactory bulb with its precisely organized glomeruli (Belluscio *et al.* 2002; Aungst *et al.* 2003) can be considered a functional whole, a sense organ, in analogy with the eye, which includes an optical part and a retina consisting of a photoreceptor layer connected to a complex neuronal circuitry. Here, we focus on the size of the olfactory organ. Absolute size may be of crucial functional importance as the mammalian ability to discriminate between thousands of odours relies on a multigene family encoding about 1000 different olfactory receptor molecules (Buck & Axel 1991), and the task of the bulb and the rest of the central olfactory system is to compare signals among millions of odorant receptor cells (Mori *et al.* 1999).

The epithelia in a mammalian nasal cavity cover a complex system of plates and rolls of bone and cartilage, and only a careful histological study of soft tissues can tell us which parts of the epithelia serve olfaction. Thus, skeletal material cannot be directly used for estimating the area of the olfactory epithelium and thereby the olfactory organ size (OOS). The same applies to the volume of the olfactory bulb. However, the imprint formed by the olfactory bulb into the ethmoid bone is generally well preserved, and can be readily studied in a quantitative manner as was done in the pioneering study by Bhatnagar & Kallen (1974). We have made endocranial casts of the frontal skull region where the ethmoid bone (the cribriform plate) forms a shallow elliptic depression, or sometimes a deeper cavity (figure 1*a*,*b*). In the endocasts, the perforated region of the ethmoid bone (referred to here simply as 'the ethmoid') appears as a granulate surface. The area of this surface corresponds to the bulb area receiving olfactory nerve bundles.

2. MATERIAL AND METHODS

(a) *Skull material and taxonomy*

The study is based on 244 skulls representing 150 mammalian species and 130 genera. A majority of the skulls are at the Zoological Museum of the University of Helsinki, two are at the Natural History Museum in Stockholm, while three of the four human skulls are at the Institute of Biomedicine at the University of Helsinki. A few skulls are in the private collections of Henry Pihlström and Mikael Fortelius, respectively. The goal was to cover the vast mammalian size range and to include species representing many different systematic groups and ecological specializations, including aquatic mammals. Thus, both sirenians and the aquatic carnivores traditionally known as 'pinnipeds' (Bininda-Emonds & Gittleman 2000) are represented in the sample. However, whales are not; although cetacean embryos develop olfactory bulbs, adult specimens have no or only rudimentary bulbs and lack a perforated ethmoid bone (Oelschläger 1989).

(b) *Endocranial casts*

For casts, we used vinamold (softness 1; Bang & Bonsomer; www.bangbonsomer.fi). If not stretched, a piece of this elastic material retains its shape. When heated, it becomes fluid and a suitable amount can then be poured through the foramen magnum into the foremost part of the skull where it

* Author for correspondence (henry.pihlstrom@helsinki.fi).

Received 5 February 2004
Accepted 25 October 2004

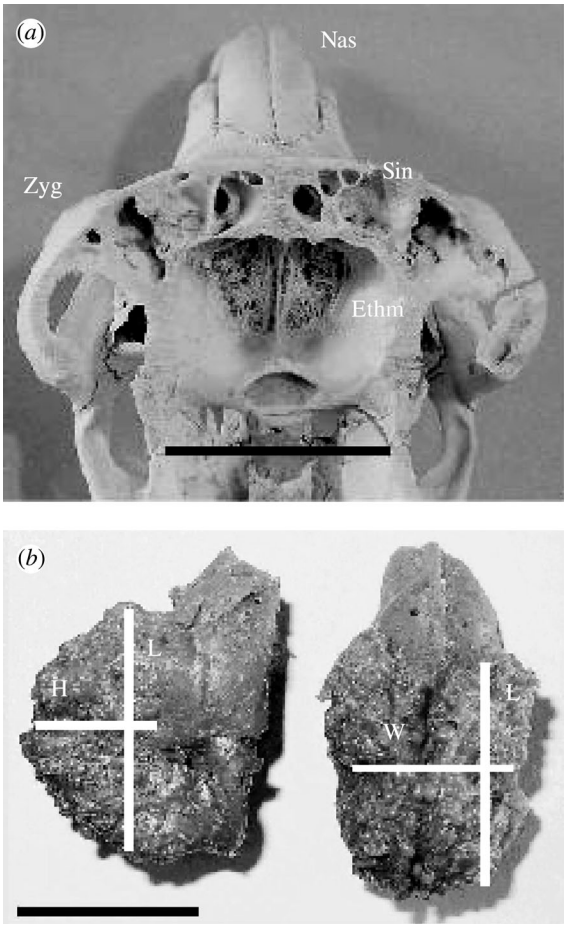

Figure 1. (*a*) Dorso-caudal view of the skull of a mouflon sheep *Ovis aries* (HP) with the skull roof removed. Scale bar, 50 mm. Ethm, cribriform plate of ethmoid (ethmoid bone); Nas, nasal bone; Sin, transect of the skull roof showing non-olfactory sinus cavities; Zyg, zygomatic arch. In ungulates, the bulb is divided and the left and right halves are treated as two ellipsoids. (*b*) Vinamold endocasts of the ethmoid bones of two wolves *Canis lupus* (FMNH 34 651 left; FMNH 39 569 right). Left cast seen laterally, with the nasal cavity side turned to the left and the brain side turned to the right. Right cast seen frontally, with the nasal cavity side turned towards the viewer. Black scale, 20 mm. *H*, height of perforated area; *L*, length of perforated area; *W*, width of perforated area (see §2). In canids, the bulb is undivided and treated as one compact ellipsoid.

fills the cavities originally surrounding the olfactory bulb (figure 1*a*,*b*). After cooling, the solid but elastic cast was carefully detached and then lifted out through the foramen magnum. All ethmoid casts are stored in the private collection of HP.

(c) *Measurement and calculation of ethmoid and skull areas*

The same person (HP) took all measurements, using digital callipers. The perforated part of the ethmoid bone is represented by a granulate region on the surface of the vinamold cast, with each 'grain' representing a hole. The curved area of this region can be determined using different direct methods (Bhatnagar & Kallen 1974). However, we have used a calculation method intended to minimize subjective judgements and maximizing reproducibility.

Let a plane cut the endocast along the edge of the grainy area. The plane surface circumscribed by the cut edge is assumed to be an ellipse of a longer axis L (length) and a shorter axis W (width). The length L is measured as the longest dimension of this imagined elliptic surface, and the shorter axis W is measured perpendicularly as the width of the perforated area at the centre of L (figure 1*b*, right). The area of such an ellipse is $\pi LW/4$. However, the grainy area is larger owing to its curvature, and a measure of this effect is needed. The height H of the grainy segment is measured perpendicularly to the elliptic surface at the centre of L (see figure 1*b*, left).

Based on these three measurements of L, W and H, the grainy area is calculated. We assume that the shape of this area is a segment of a spheroid, that is, an ellipsoid with two axes of equal length $2b$ and an axis of revolution of a length $2a$. The equation describing such a spheroid is

$$x^2/a^2 + y^2/b^2 + z^2/b^2 = 1. \tag{2.1}$$

If b is larger than a, then the spheroid is oblate, that is, flattened out along the x-axis (discus type). If b is smaller than a, then this spheroid is prolate, that is, stretched out along the x-axis (cigar type).

When the plane $z=z_o$ cuts from this spheroid an ellipse with axes L and W, the thickness of the spheroid segment is $H=b-z_o$. A segment of length L, width W and height H could be fitted both to an oblate and to a prolate spheroid segment. The area of an oblate segment is smaller than the corresponding prolate segment, especially in deep segments. In species characterized by a deep segment (e.g. *Canis* species, red fox and northern fur seal), the shapes of the endocasts were clearly more of the oblate type, where the curvature in the direction L is an arc of a circle and the curvature in the direction W is an arc of an ellipse. Thus, we calculated all areas assuming oblate ellipsoids.

Using L, W and H, the axes b and a are

$$b = 1/2(L^2/4 + H^2)/H, \quad a = bW/L. \tag{2.2}$$

Because the ellipse with axes L and W is a projection of the segment surface to the x, y-plane, the segment area is an integral over that projection area,

$$A = \int \mathrm{d}A'/\cos\varphi, \tag{2.3}$$

where $\mathrm{d}A' = \mathrm{d}x\mathrm{d}y$ is a projection of a segment surface element $\mathrm{d}A$ to the x, y-plane, and $\varphi(x, y)$ is an angle between the x, y-plane and the segment surface element $\mathrm{d}A$. According to equation (2.1),

$$z = b\sqrt{1 - x^2/a^2 - y^2/b^2}, \tag{2.4}$$

$\tan\varphi$ is the magnitude of the gradient of this function,

$$\tan\varphi = \sqrt{(e^4x^2 + y^2)/(b^2 - e^2x^2 - y^2)}. \tag{2.5}$$

Here, $e=L/W$. The segment areas were calculated with the MATLAB program as the surface integrals

$$A = 4\int_0^{W/2} \mathrm{d}x \int_0^{L/2\sqrt{1-4x^2/W^2}} \mathrm{d}y/\cos\varphi. \tag{2.6}$$

The olfactory bulb, like most compartments of the brain, is a paired organ. However, usually the left and right halves and the corresponding cast form one compact body, which is best treated as one ellipsoid (figure 1*b*). In some species such as all ungulates, the two bulb halves and the corresponding cast form two separated ellipsoids (figure 1*a*). In these cases, we calculated the areas of both and used the sum of them. The separation of the bulb into two halves is an anatomical

Table 1. Areas of ethmoids and olfactory epithelia of 16 mammalian species.
(For epithelium area values, only studies based on cross-sections through the whole nose are considered; when a species is described in several studies, the results are averaged.)

species	ethmoid area (mm^2) (*n*)	log ethmoid area (mm^2)	epithelium area (mm^2)	log epithelium area (mm^2)	references
eastern hedgehog *Erinaceus concolor*	114 (1)	2.057	1960	3.292	Sigmund & Sedláček (1985)
common shrew *Sorex araneus*	12.5 (1)	1.097	199	2.299	Gurtovoi (1966), Söllner & Kraft (1980) and Sigmund & Sedláček (1985)
water shrew *Neomys fodiens*	12.1 (1)	1.083	94.4	1.975	Söllner & Kraft (1980)
Jamaican fruit bat *Artibeus jamaicensis*	17.3 (1)	1.238	232	2.365	Bhatnagar & Kallen (1975)
mouse-eared bat *Myotis myotis*	8.2 (1)	0.914	188	2.274	Kolb (1971)
lesser mouse-eared bat *Myotis blythii*	7 (1)	0.845	68.4	1.835	Gurtovoi (1966)
noctule *Nyctalus noctula*	7.4 (1)	0.869	176	2.246	Kolb (1971)
brown long-eared bat *Plecotus auritus*	5.9 (1)	0.771	35.1	1.545	Kolb (1971)
human *Homo sapiens*	132 (4)	2.121	1125	3.051	Negus (1958)
dog (German shepherd) *Canis familiaris*	578 (1)	2.762	13 900	4.143	Lauruschkus (1942)
cat *Felis catus*	89.5 (2)	1.952	2791	3.446	Lauruschkus (1942) and Negus (1958)
wild boar *Sus scrofa*	1940 (1)	3.288	28 800	4.459	Güntherschulze (1979)
roe deer *Capreolus capreolus*	588 (1)	2.769	9000	3.954	Kolb (1975)
deer mouse *Peromyscus maniculatus*	13.2 (2)	1.121	167	2.223	Adams (1972)
bank vole *Clethrionomys glareolus*	9.14 (13)	0.961	160	2.204	Gurtovoi (1966)
rabbit *Oryctolagus cuniculus*	68 (2)	1.833	832	2.920	Negus (1958), Allison & Warwick (1949), Mulvaney & Heist (1970) and Adams (1972)

feature increasing the area to which olfactory axons can project. High *H* values serve the same end (figure 1*b*).

Bhatnagar & Kallen (1974) studied the ethmoid bones of 40 species of bats, and using camera lucida tracings, they measured the areas of the perforated portions. Five of their species are also included in our sample. The areas given by them are as follows (with our data in brackets): *Glossophaga soricina* 3.6 (7.8), *Phyllostomus discolor* 6.9 (14.9), *Carollia perspicillata* 7.9 (13.3), *Artibeus jamaicensis* 11.7 (17.3) and *Desmodus rotundus* 7.3 (14.9) mm^2. Compared with their data our areas are about two times larger. The reason for this is methodological: Bhatnagar and Kallen used planar projections and circumscribed the perforated regions very narrowly and further excluded a non-perforated area in the middle. However, the consistent relation between their areas and ours is encouraging as it means that species differences observed by them are also found in our study.

In addition to the ethmoid area, we use a quadrative measure for the size of the skull. It was obtained by multiplying the length (mm) of the skull (from the tip of the nose to the back border of foramen magnum) with the width of the cranial base, and in the text, it is referred to as 'skull area'.

3. RESULTS

For 16 out of the 150 species investigated here, we have found histological studies describing the olfactory epithelia and their areas (table 1; Lauruschkus 1942; Allison & Warwick 1949; Negus 1958; Gurtovoi 1966; Mulvaney & Heist 1970; Kolb 1971, 1975; Adams 1972; Bhatnagar & Kallen 1975; Güntherschulze 1979; Söllner & Kraft 1980; Sigmund & Sedláček 1985). By relating the areas of the epithelia to the corresponding ethmoid areas determined in our study, we test the hypothesis that the olfactory organ is a functional whole with rather constant geometric relations (figure 2). The function describing the ethmoid/epithelium area relation does not significantly deviate from isometry (figure 2, caption). The olfactory epithelium is typically 16 times larger than the ethmoid area. The human data point is in the middle, together with middle-sized mammals like the rabbit, the cat and the hedgehog, and far below more human-sized animals like the German shepherd dog, the roe deer and the wild boar. Thus, the isometry observed is not a result of general mammalian skull isometry, but of constant geometric relations within the olfactory organ. Obviously, the ethmoid is indeed a good and accessible OOS indicator.

For relating OOS to animal size, the log area of the ethmoid is plotted as a function of log 'skull area'; the line is the least-squares regression describing all species included (figure 3, caption). As a general tendency for the whole dataset, the ethmoid/skull relation is weakly negatively allometric. Some olfactory specializations within the class Mammalia are indicated by choosing three more or less non-overlapping orders, Chiroptera, Primates and Artiodactyla, and marking them with different symbols. Bats and artiodactyls do not significantly deviate from the regression line where their olfactory organs are roughly proportional to skull size. Among the primates, the prosimians have olfactory organs typical for animals of their size (open circles close to the regression line). However, human, apes and monkeys clearly lie below the line. A reduced role of olfaction in primates is also indicated by the observation that 50–70% of the olfactory receptor genes are non-functional in humans, with a somewhat lower percentage in apes and the rhesus macaque (*Macaca mulatta*; Rouquier *et al.* 2000; Gilad *et al.* 2003). Ethmoid/skull ratios can be seen

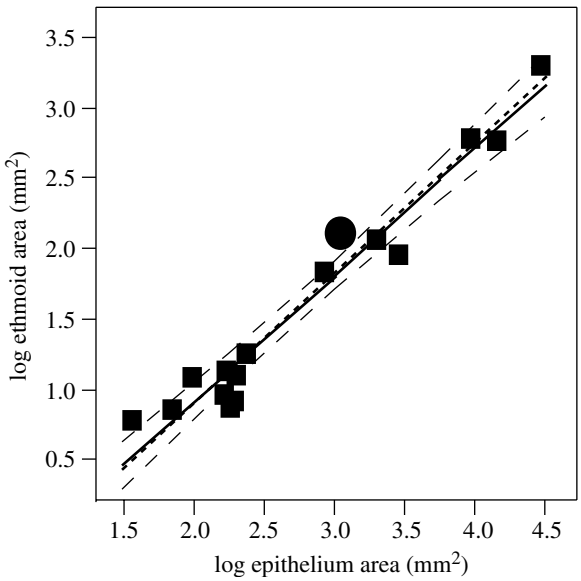

Figure 2. Regression of log-transformed ethmoid bone area on olfactory epithelium area (both in mm^2). The least-squares regression equation is

$$\log(\text{ethmoid area}) = -0.883 + 0.900 \log(\text{epithelial area})$$

($n=16$, $r^2=0.953$). The apparent weak negative allometry is not significantly different from isometry (95% confidence intervals of regression coefficient 0.790–1.004). Dashed lines show 95% confidence limits of the least-squares fit; the dotted line is the major axis regression line. Big solid circle shows *Homo sapiens*. Data are from table 1.

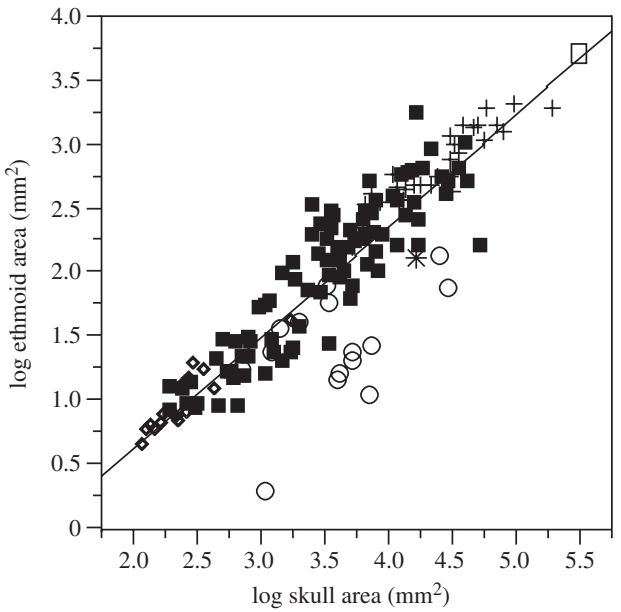

Figure 3. Regression of log-transformed ethmoid bone area on skull area (both in mm^2). The least-squares regression equation is

$$\log(\text{ethmoid area}) = -1.119 + 0.871 \log(\text{skull area})$$

($n=150$, $r^2=0.815$). The relationship is weakly but significantly negatively allometric (95% confidence interval of regression coefficient 0.821–0.919). Using maximum, rather than basal skull length for primates, including *Homo*, does not change the relationship significantly. Without primates the regression equation is

$$\log(\text{ethmoid area}) = -1.122 + 0.891 \log(\text{skull area})$$

($n=134$, $r^2=0.908$, 95% confidence intervals of regression coefficient 0.851–0.933). Symbol coding: diamonds, bats; open circles, primates; crosses, artiodactyls. The asterisk and open square show *Homo sapiens* and *Elephas maximus*, respectively. Complete data can be found in the Electronic Appendix.

as anatomical criteria for olfactory specialization. The four species with the highest ratios are the nine-banded armadillo, the aardvark, the two-toed sloth and the striped skunk. The four lowest ratios are those of two monkeys (the guereza and the red-handed tamarin), the orangutan and the dugong. The Electronic Appendix provides taxonomic data and number of specimens per species, and lists ethmoid and skull areas.

4. DISCUSSION

In large terrestrial mammals, the sizes of the eyes and ears are limited by functional constraints or anatomical and ecological cost/benefit restrictions (Quiring 1950; Hughes 1977; Hemilä *et al.* 1995; Nummela 1995). In olfaction we see no obvious size saturation. The Asian elephant, the black rhinoceros and the big artiodactyls (with the exception of the hippopotamus) seem to have very large olfactory organs proportional to their big skulls (figure 3). In agreement with our ethmoid data, a macroscopic dissection of the Asian elephant shows very large ethmoturbinals in the nasal cavity (Boas & Paulli 1925). Another question is to what degree organ size and/or ethmoid/skull quotients correlate with sensitivity and discrimination. Quantitative threshold data exist for human and canine olfaction, as well as for some monkeys and bats and a few other relatively small mammals. For a number of volatile substances, the threshold concentrations for dogs are 1/100–1/10 000 of human threshold concentrations (Neuhaus 1953; Moulton & Marshall 1976; Marshall *et al.* 1981). We also note that pigs and wild boars are said to outperform dogs in demanding olfactory tasks (Güntherschulze 1979). In these cases, a higher olfactory sensitivity correlates with a larger organ. This can be compared with the hedgehog/human relation since hedgehogs have human-sized olfactory epithelia and ethmoids (figure 2), and human-like thresholds (Bretting 1972).

According to Laska & Seibt (2002) anatomical criteria may be misleading when we compare the olfactory performances of two different mammalian species, for instance, rats and macaque monkeys. This criticism is partly justified but the problem should be further specified. It is evident that, as a response to different evolutionary pressures, each species has its own olfactory profile, and thus we cannot define and quantify a universal olfactory capacity (Laska & Seibt 2002). Moreover, in case we use OOS as an anatomical criterion, we must differ between absolute and relative size. Rats and pigtail macaques (*Macaca nemestrina*) have, on an average, similar sensitivities to 1-alcohols (Laska & Seibt 2002), and their olfactory organs are apparently of similar size. We have no data for the ethmoid of the pigtail macaque but we note that the ethmoids of the Barbary macaque (*Macaca sylvanus*) and the rat are similar (27 and 21 mm^2, respectively). However, their ethmoid/skull ratios are clearly different (0.004 and 0.030, respectively), and relative to skull size, the rat has a much larger olfactory organ.

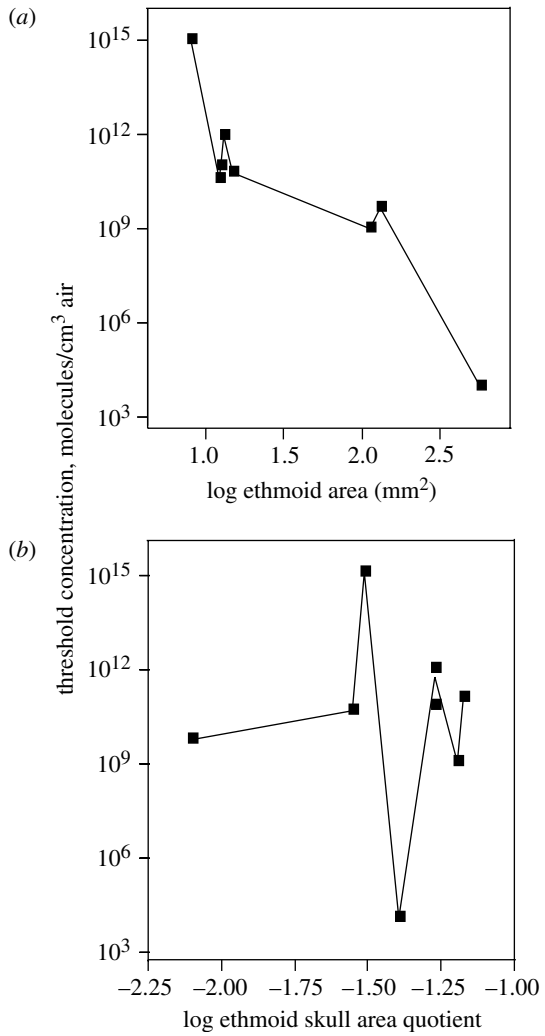

Figure 4. Absolute thresholds to butyric acid plotted as function of (*a*) log ethmoid area; (*b*) log ethmoid/skull area quotient. The species (and reference to threshold data), from smaller to larger ethmoids: *Myotis myotis* (Obst & Schmidt 1976), *Phyllostomus discolor* (Schmidt 1975), *Sorex araneus* (Sigmund & Sedláček 1985), *Carollia perspicillata* (Laska 1990), *Desmodus rotundus* (Schmidt 1975), *Erinaceus europaeus* (Bretting 1972), *Homo sapiens* (Bretting 1972), *Canis familiaris*, German shepherd (Moulton & Marshall 1976).

The above results indicate that absolute olfactory thresholds appear to be related to absolute OOS, but not to ethmoid/skull quotient. This tendency is best seen by plotting, for eight mammalian species, the thresholds to butyric acid (Neuhaus 1953; Schmidt 1975; Obst & Schmidt 1976; Sigmund & Sedláček 1985; Laska 1990) as a function of both absolute ethmoid area and ethmoid/skull ratio (figure 4*a*,*b*). The log thresholds drop fairly consistently, although not monotonically, as a function of log ethmoid area. By contrast, there is no consistent tendency in the plot of threshold versus ethmoid/skull ratio. A high ethmoid/skull ratio indicates that olfaction is important in the sensory ecology of a given species, but it does not guarantee a low threshold to a randomly selected odorant.

The thresholds to butyric acid drop by about 10 orders of magnitude while the ethmoid area increases by a factor of only 70 (figure 4*a*). Similar observations have been made for a number of common metabolites (Schmidt 1975; Sigmund & Sedláček 1985). The mechanism behind these huge sensitivity differences is unknown. Apparently, the differences are not related to different sensory cell densities in the epithelia. For humans, dogs and most other mammals, the densities are fairly constant, roughly 2×10^4 receptor cells mm^{-2} (Güntherschulze 1979). Very low thresholds could possibly be obtained by large olfactory organs, which, in addition to many types of specialized sensory cells, would also have sensitive and less specific cells serving more general detection tasks. Consistent with this hypothesis, are the extended stimulus-response functions describing olfactory performance in dogs. They indicate cooperation of several classes of olfactory sensory cells with different but overlapping ranges of absolute sensitivity (Moulton & Marshall 1976; Marshall *et al*. 1981).

In this study, we show that, as a general tendency for the whole material, the size of the olfactory organ is roughly proportional to skull size. By relating our anatomical observations to available threshold data, we find that large absolute organ size tends to favour high sensitivity. This parallels the anatomy of vision in diurnal birds and mammals for which absolute eye size limits acuity, independent of the size of the skull and the brain (Hughes 1977).

We thank Kristian Donner for valuable comments. This work was supported by a grant from Oskar Öflunds Stiftelse.

REFERENCES

Adams, D. R. 1972 Olfactory and non-olfactory epithelia in the nasal cavity of the mouse, *Peromyscus*. *Am. J. Anat.* **133**, 37–50.

Allison, A. C. & Warwick, T. T. 1949 Quantitative observations on the olfactory system of the rabbit. *Brain* **72**, 186–197.

Aungst, J. L., Heyward, P. M., Puche, A. C., Karnup, S. V., Hayar, A., Szabo, G. & Shipley, M. T. 2003 Centre-surround inhibition among olfactory bulb glomeruli. *Nature* **426**, 623–629.

Belluscio, L., Lodovichi, C., Feinstein, P., Mombaerts, P. & Katz, L. C. 2002 Odorant receptors instruct functional circuitry in the mouse olfactory bulb. *Nature* **419**, 296–300.

Bhatnagar, K. P. & Kallen, F. C. 1974 Cribriform plate of ethmoid, olfactory bulb and olfactory acuity in forty species of bats. *J. Morphol.* **142**, 71–90.

Bhatnagar, K. P. & Kallen, F. C. 1975 Quantitative observations on the nasal epithelia and olfactory innervation in bats. *Acta Anat.* **19**, 272–282.

Bininda-Emonds, O. R. P. & Gittleman, J. L. 2000 Are pinnipeds functionally different from fissiped carnivores? The importance of phylogenetic comparative analyses. *Evolution* **54**, 1011–1023.

Boas, T. E. V. & Paulli, S. 1925 *The elephant's head, part 2*. Copenhagen: The Carlsberg Fund.

Bretting, H. 1972 Die Bestimmung der Riechschwellen bei Igeln (*Erinaceus europaeus* L.) für einige Fettsäuren. *Z. Säugetierk.* **37**, 286–311.

Buck, L. & Axel, R. 1991 A novel multigene family may encode odorant receptors: a molecular basis for odor recognition. *Cell* **65**, 175–187.

Gilad, Y., Man, O., Pääbo, S. & Lancet, D. 2003 Human specific loss of olfactory receptor genes. *Proc. Natl Acad. Sci. USA* **100**, 3324–3327.

Güntherschulze, J. 1979 Studien zur Kenntnis der Regio olfactoria von Wild- und Hausschwein (*Sus scrofa scrofa* L. 1768 und *Sus scrofa f. domestica*). *Zool. Anz. Jena* **202**, 256–279.

Gurtovoi, N. N. 1966 Ecological–morphological differences in the structure of the nasal cavity in the representatives of the orders Insectivora, Chiroptera and Rodentia. *Zool. Zh.* **45**, 1536–1550. [In Russian with English summary.]

Hemilä, S., Nummela, S. & Reuter, T. 1995 What middle ear parameters tell about impedance matching and high frequency hearing. *Hear. Res.* **85**, 31–44.

Hughes, A. 1977 The topography of vision in mammals of contrasting life style: comparative optics and retinal organisation. In *Handbook of sensory physiology, vol. VII/5: the visual system in vertebrates* (ed. F. Crescitelli), pp. 613–756. Berlin: Springer-Verlag.

Kolb, A. 1971 Licht- und elektronenmikroskopische Untersuchungen der Nasenhöhle und des Riechepithels einiger Fledermausarten. *Z. Säugetierk.* **36**, 202–213.

Kolb, A. 1975 Lichtmikroskopische Untersuchungen am Riechepithel des Rehes (*Capreolus capreolus*). *Anat. Anz.* **137**, 417–428.

Laska, M. 1990 Olfactory sensitivity to food odor components in the short-tailed fruit bat, *Carollia perspicillata* (Phyllostomidae, Chiroptera). *J. Comp. Physiol. A* **166**, 395–399.

Laska, M. & Seibt, A. 2002 Olfactory sensitivity for aliphatic alcohols in squirrel monkeys and pigtail macaques. *J. Exp. Biol.* **205**, 1633–1643.

Lauruschkus, G. 1942 Über Riechfeldgröße und Riechfeldkoefficient bei einigen Hunderassen und der Katze. *Arch. Tierheilk.* **77**, 473–497.

Marshall, D. A., Blumer, L. & Moulton, D. G. 1981 Odor detection curves for *n*-pentanoic acid in dogs and humans. *Chem. Senses* **6**, 445–453.

Mori, K., Nagao, H. & Yoshihara, Y. 1999 The olfactory bulb: coding and processing of odor molecule information. *Science* **286**, 711–715.

Moulton, D. G. & Marshall, D. A. 1976 The performance of dogs in detecting α-ionone in the vapor phase. *J. Comp. Physiol.* **110**, 287–306.

Mulvaney, B. D. & Heist, H. E. 1970 Mapping of rabbit olfactory cells. *J. Anat.* **107**, 19–30.

Negus, V. 1958 *The comparative anatomy and physiology of the nose and paranasal sinuses*. Edinburgh and London: E. & S. Livingstone.

Neuhaus, W. 1953 Über die Riechschärfe des Hundes für Fettsäuren. *Z. Vergl. Physiol.* **35**, 527–552.

Nummela, S. 1995 Scaling of the mammalian middle ear. *Hear. Res.* **85**, 18–30.

Obst, Ch. & Schmidt, U. 1976 Untersuchungen zum Riechvermögen von *Myotis myotis* (Chiroptera). *Z. Säugetierk.* **41**, 101–108.

Oelschläger, H. A. 1989 Early development of the olfactory and terminalis systems in baleen whales. *Brain Behav. Evol.* **34**, 171–183.

Quiring, D. P. 1950 *Functional anatomy of the vertebrates*. New York: McGraw-Hill.

Rouquier, S., Blancher, A. & Giorgi, D. 2000 The olfactory receptor gene repertoire in primates and mouse: evidence for reduction of the functional fraction in primates. *Proc. Natl Acad. Sci. USA* **97**, 2870–2874.

Schmidt, U. 1975 Vergleichende Riechschwellenbestimmungen bei neotropischen Chiropteren (*Desmodus rotundus*, *Artibeus lituratus*, *Phyllostomus discolor*). *Z. Säugetierk.* **40**, 269–298.

Sigmund, L. & Sedláček, F. 1985 Morphometry of the olfactory organ and olfactory thresholds of some fatty acids in *Sorex araneus*. *Acta Zool. Fennica* **173**, 249–251.

Söllner, B. & Kraft, R. 1980 Anatomie und Histologie der Nasenhöhle der Europäischen Wasserspitzmaus, *Neomys fodiens* (Pennant 1771), und anderer mitteleuropäischer Soriciden. *Spixiana* **3**, 251–272.

The supplementary Electronic Appendix is available at http://dx.doi.org/10.1098/rspb.2004.2993 or via http://www.journals.royalsoc.ac.uk.